28.06.2020

Furkan Tokgöz

EE568

Project-4

Axial-flux Permanent Magnet Synchronous Machine with Unequal Width Radial Winding PCB

1) Literature Review

Axial-flux machines have been becoming more and more popular everyday thanks to their short axial-length, higher torque and power densities. However, axial-flux machines are not very suitable for mass production purposes, because of their planar stator geometry which makes the production of the stator challenging. PCB motor offers a solution to this problem by the use of the precise and cheap manufacturing options of printed circuit board technology that enables AFPMSM with PCB winding to be used in small wind-turbines, water current turbines, hard-disk drives, video disk drives and spindle motors [1-5].

Fast and cheap PCB manufacturing process ensures that all printed circuit boards can be produced with precision in micrometres range which facilitates construction of small electric motors. Control algorithms such as model predictive control or direct torque control requires motor parameters to be known. After designing the printed circuit board, stator parameters can be calculated using finite element analysis tools. Since, every PCB will be identical to each other, thanks to the manufacturing precision, these control methods can accurately be implemented into the design. Moreover, there is no cogging torque due to air-cored stator structure. Lastly, PCB motors have fewer number of turns and large effective air gap which make the phase inductances low. The lower the inductance, the smaller the electrical time constant and the better the transient performance.

In literature, there are different winding designs for PCB motors. The concentric winding which is a very commonly used winding type, has a high induced voltage and torque output because of high flux linking area and long radial winding length. However, end winding connections of the concentric winding is long. As a result, resistance of the current path increases, so the thermal stress of stator windings is high and the efficiency of the motor is low. Alternatively, wave winding topologies are proposed in [6]. The main purpose in design is to increase the efficiency of the winding without losing the dynamic performance of the motor. A comparison of different windings for PCB motors are presented in [7], but it should be noted that PCB inner and outer diameters of various windings are chosen differently and fractional pitched stator coils are used.

2) Analytical Calculation & Sizing

In this project, I have designed a double rotor-single stator permanent magnet axial-flux synchronous machine with PCB winding. In order find have better understanding about the analysis, which is presented in this report, I have tried to make a comparative analysis of an AFPMSM with PCB winding which is designed in [3]. The spindle motor designed in [3], is a single-sided AFPMSM with a stator which has rhomboidal winding configuration. The thickness of the motor is 3 mm and inner and outer diameters are 5.8 and 15.8 mm respectively. I have tried to make the two motor designs as close as possible. However, the major difference between two designs is that the stator winding, which is designed in [3], has rhomboidal winding configuration. The main reason why the rhomboidal winding is used in [3] is that conventional winding design results in long end winding connections which causes the efficiency of the motor to fall down. Rhomboidal winding utilizes the end winding connections by simply rotating the whole winding 90 degrees. This way end winding connections are shortened and the efficiency of the motor is increased.

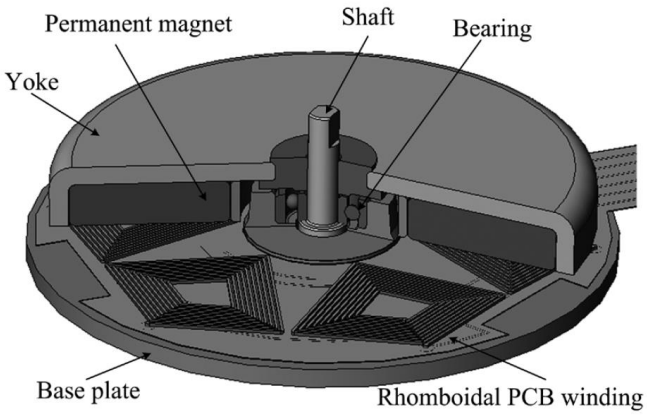

Figure 1. Spindle motor with rhomboidal winding [3].

However, the major disadvantage of this configuration is that PCB surface area is not utilized successfully. Moreover, areas of the flux linking coils are not the same for every turn in the winding. Also, output torque of this machine will not be very high since traces are positioned with an angle. For this purpose, I have designed an unequal width radial winding. Radial winding offers the maximum amount of torque that can be extracted from the machine. Unequal width offers the minimum electrical and thermal resistance and maximum utilization of the PCB surface area.

So, I have designed the PCB which can be seen in Fig.2. There are 42 slots, 3 phase and 14 poles. So, slot/pole/phase becomes 1. The winding factor of the machine 1. Phasor representation of the voltage vector can be seen in Fig.3. The PCB has 2 layers. Both top and bottom layers of the PCB is used to create a loop for the winding.

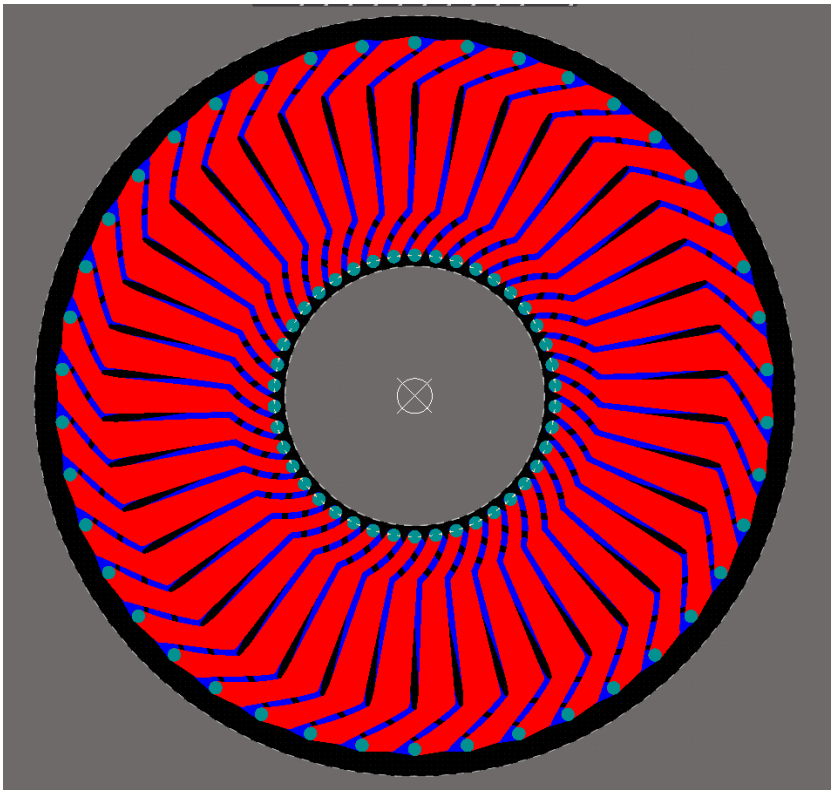

Figure 2. Unequal width radial winding design.

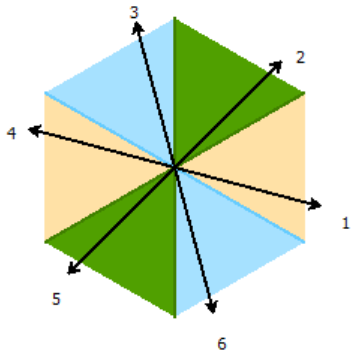

Figure 3. Star of slot representation of the designed winding.

Since, motor is very small, I had to check the limitations of the PCB producers. As can be seen in Fig. 4, the minimum thickness of the PCB in 0.2 mm. In reference design it was chosen as 0.1 mm. I have tried to decrease the clearance between traces and I have used 1 oz/ft^2 copper on traces.

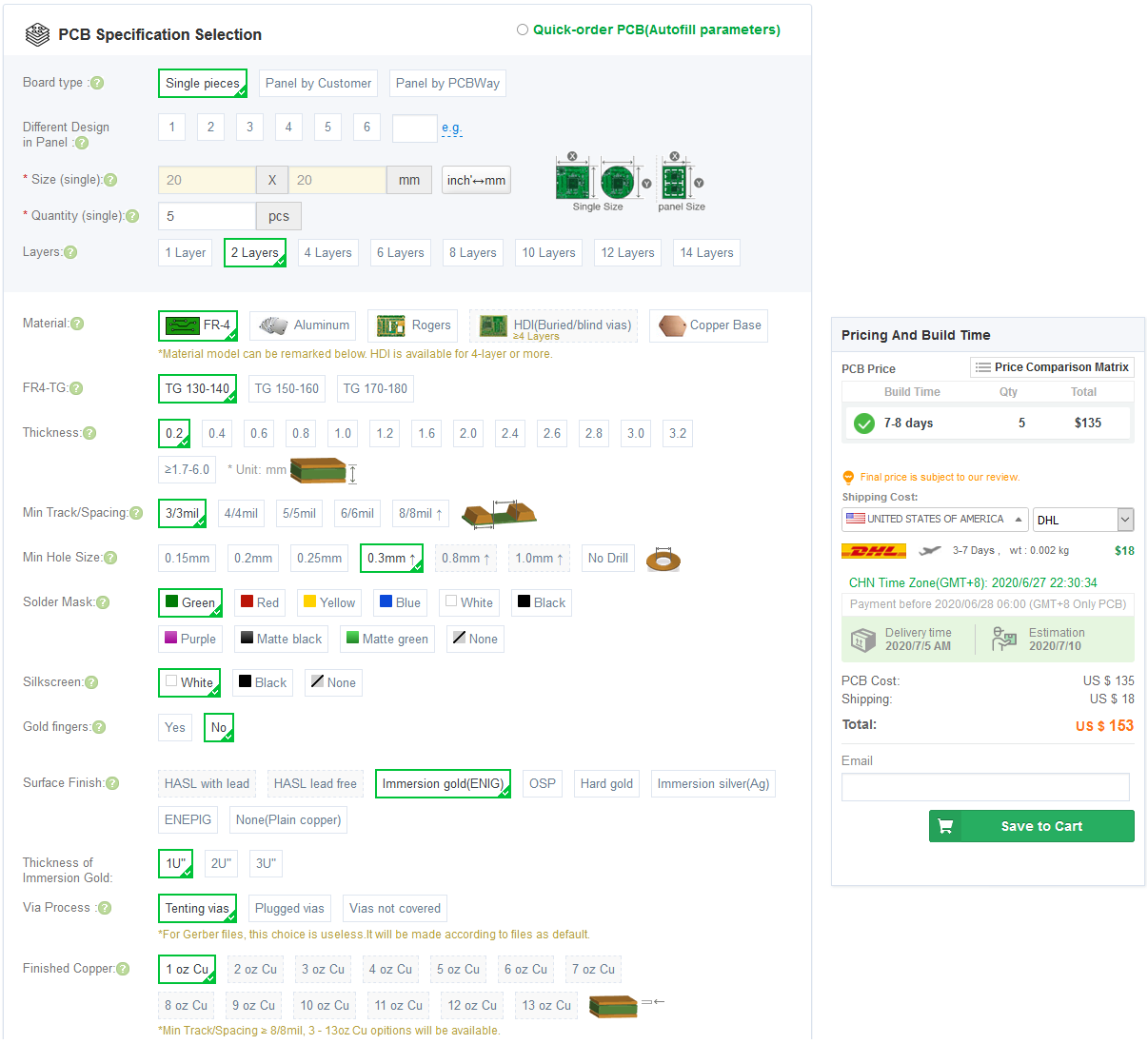

Figure 4. Limitations of the PCB production.

In reference design, single rotor single stator design is used but I have used double rotor-single stator configuration. The reason why I have used this topology is that the speed of the motor is high as 12500 RPM. The eddy current losses at this speed would be dominating the performance of the motor. When double rotor configuration is used both of the rotor yokes will rotate at the same speed so that there will be no eddy current induced on the rotor yokes. I have tried to make the motor as similar as possible to the reference design to see the difference between each winding more clearly. The detailed motor parameters can be seen in Table 1.

Table 1. Parameters of the designed motor.

Outer diameter	15.8 mm	***Air gap length***	0.4 mm
Inner diameter	6.3 mm	***PCB thickness***	0.2 mm
Thickness of motor	5 mm	***Number of slots***	42
Number of poles	14	***Copper thickness***	1 oz/ft^2
Speed	12500 RPM	***Back core thickness***	0.6 mm
$I_{full\text{-}load}$	0.5 A	***Magnet thickness***	1.4 mm

I have used N42 grade, with 1.33 T residual flux density value, NdFeB permanent magnet which is shaped as sectors to have maximum use of rotor surface. Thickness of the magnets are 1.4 mm same as [3]. The motor can be represented as in Fig.5.

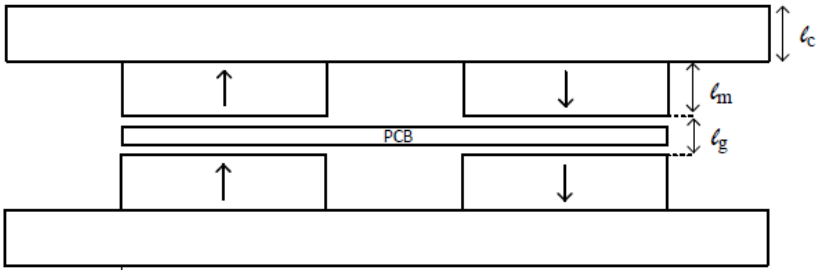

Figure 5. Representation of the double rotor-single stator axial-flux permanent magnet motor.

So, peak flux density of the air gap can be calculated as follows

$$B_{peak} = \frac{2.l_m.B_r}{2.l_m + u_r.l_g} = \frac{2.1{,}4.1{,}33}{2.1{,}4 + 1{,}05.0{,}4} = 0.967\ T$$

Assuming square shaped flux density distribution across the air gap, mean air gap flux density -magnetic loading- can be calculated as

$$\overline{\mathrm{B}} = \frac{2.B_{peak}}{\pi} = \frac{2.0{,}967}{\pi} = 0.616\ T$$

Flux per pole is calculated as follows:

$$\phi_{pole} = \frac{B_{avg}\pi\left(D_{outer}^2 - D_{inner}^2\right)}{p} = \frac{0{,}616\pi(0.0079^2 - 0.00315^2)}{14} = 7.25\ \mu Wb$$

Required back core thickness of the motor in order to have 2 T flux density at the back-cores is calculates as

$$l_{back-core} = \frac{\phi_{pole}}{2.B_{back-core}.(r_{outer} - r_{inner})} = \frac{7{,}25.10^{-6}}{2.2.(0.0079 - 0.00315)} = 0.58\ mm$$

2 T flux density at the back-core is chosen since the reference design also utilizes the back-cores to that flux density value. Back-core thickness is chosen as 0.6 mm. Next, I have calculated the induced voltage. For this purpose, flux linkage of one phase of the stator should be calculated. In Fig.6, area covered by the one loop of the coil can be seen. There are 7 loops of coil in one phase.

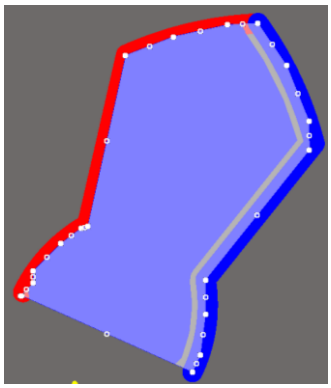

Figure 6. One loop of the coil.

So, flux linkage can be calculated as follows:

$$\lambda_{linkage} = B.A_{coil}.N = 0{,}967.11{,}141.10^{-6}.7 = 75\ \mu A$$

Induced phase voltages of the motor can be calculated as follows. Note that, since motor rotates at 12500 RPM, the frequency is 1458 Hz.

$$V_{induced-rms} = 4.44.\lambda_{linkage}.f = 4{,}44.75.10^{-6}.1458 = 0.485\ V$$

Next, electrical loading is calculated. Electrical loading in axial-flux machines is calculated at the mean radius of the stator core [8].

$$\overline{\mathrm{A}} = \frac{NIQ}{\pi D_{average}} = \frac{2.0{,}5.42}{\pi 0{,}01105} = 1210\ \mathrm{A/m}$$

Tangential stress of the motor is then calculated

$$\sigma_{tangential} = \frac{A.B}{\sqrt{2}} = 527\ Pa$$

Output torque can be calculated as follows

$$T = S_{rotor}.\sigma_{tangential}.r_{rotor} = 527.\pi(0{,}0079^2 - 0{,}00315^2).2.0{,}01105 = 1.92\ m\ N.m$$

Since, rated speed is 12500 RPM, mechanical output power can be calculated as follows

$$\omega = \frac{12500.2\pi}{60} = 1309 rad/s$$

$$P_{mech} = T.\omega = 0{,}00192.1309 = 2.5W$$

The phase resistance, if the trace width is assumed to be constant at 0.3 mm, is calculated as follows:

$$R_{phase} = \frac{\rho\ l_{trace}}{h_{trace} w_{trace}} = 0.27\ \Omega$$

Where l_{trace} is the total length of the copper trace per phase, h_{trace} is the height of the copper trace, w_{trace} is the width of the traces and ρ is the resistivity of the copper. However, the resistance will not be equal to this value since I have used unequal width winding. w_{trace} will vary as the radius changes. So, I have calculated the average width of the trace, w'_{trace}, and calculated the true resistance value.

$$R'_{phase} = R_{phase}.\frac{w'_{trace}}{w_{trace}} = 0.177\ \Omega$$

Thanks to unequal width winding the phase resistance is reduced to its 65%.

3) FEA Modelling

I have constructed the 3D model of the designed motor in ANSYS Maxwell. I have used half-symmetry to minimize the computational cost. The resulted flux density distribution at the back core can be seen in Fig.6. As expected, back-core flux density reaches up to 2 T.

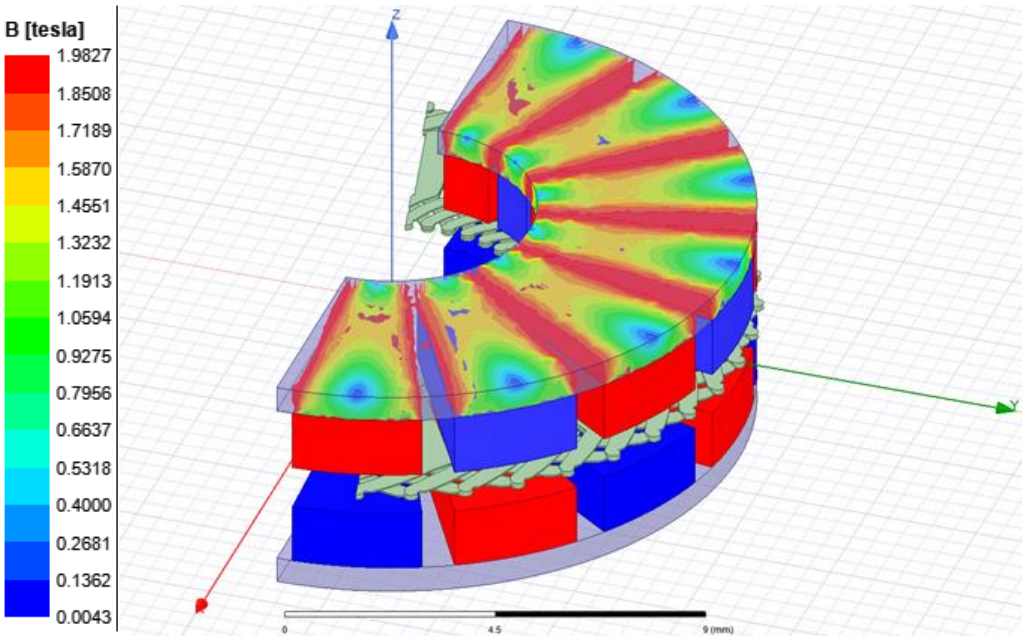

Figure 7. Magnetic flux density distribution in the back core.

Induced voltage waveforms of three phases are found as in Fig.8. The peak voltage value is found as 580 mV. In reference design, the peak induced voltage value was 200 mV with back-emf constant of 0.107 mV/(radsec). Back-emf constant of the designed motor is found as 0.443 mV/(radsec).

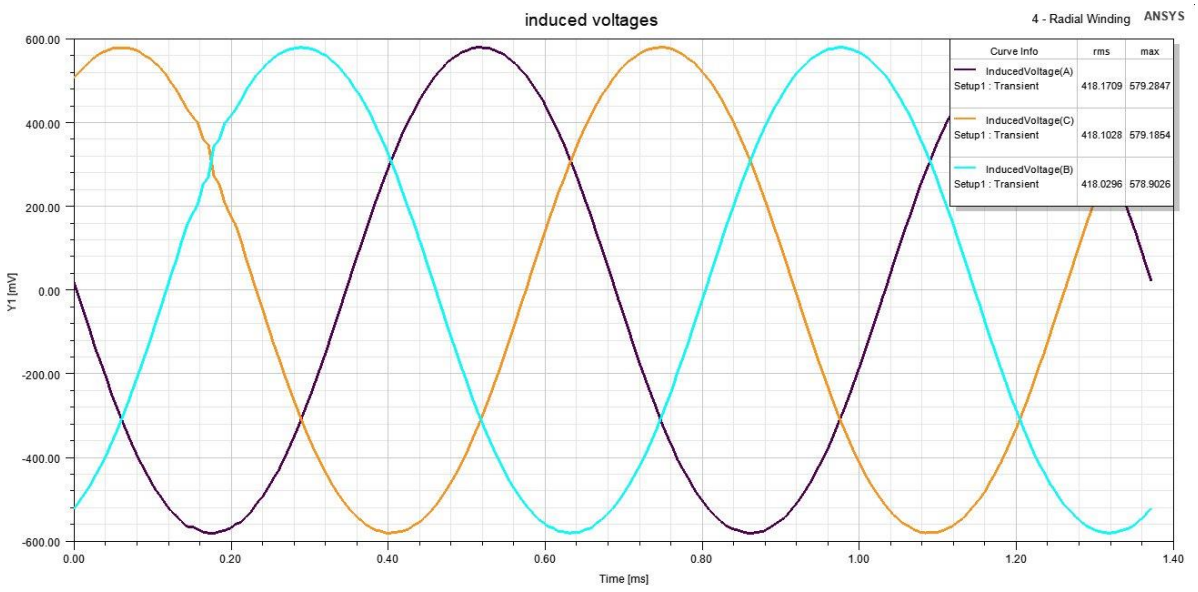

Figure 8. Induced voltage waveforms of the designed machine.

FFT of the induced voltage can be seen in Fig.9. THD of the induced voltage is calculated as 2.1%. FFT of the induced voltage of the reference design can be seen in Fig.10. THD levels are not

presented in the paper but one can observe that third harmonic is higher when it is compared to the design with the radial winding.

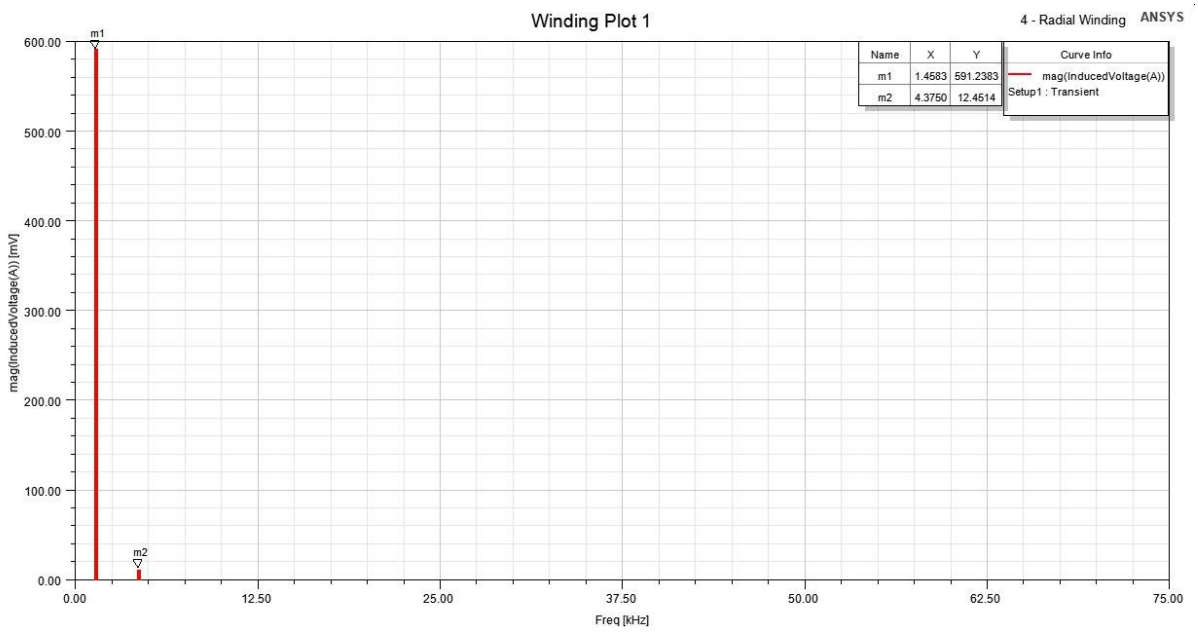

Figure 9. FFT result of the induced voltage waveform.

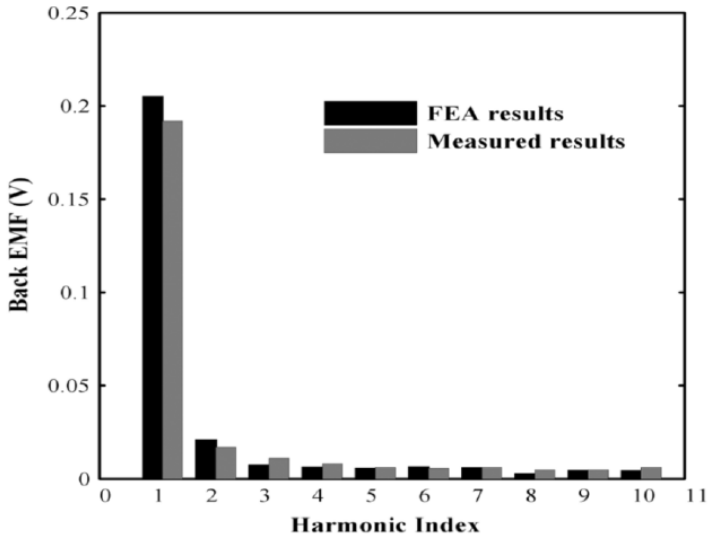

Figure 10. FFT results of the the reference design [3].

The full-load current value of 0.5 A_{rms} is chosen and applied to the terminals of the motor. The phase currents can be seen in Fig.11.

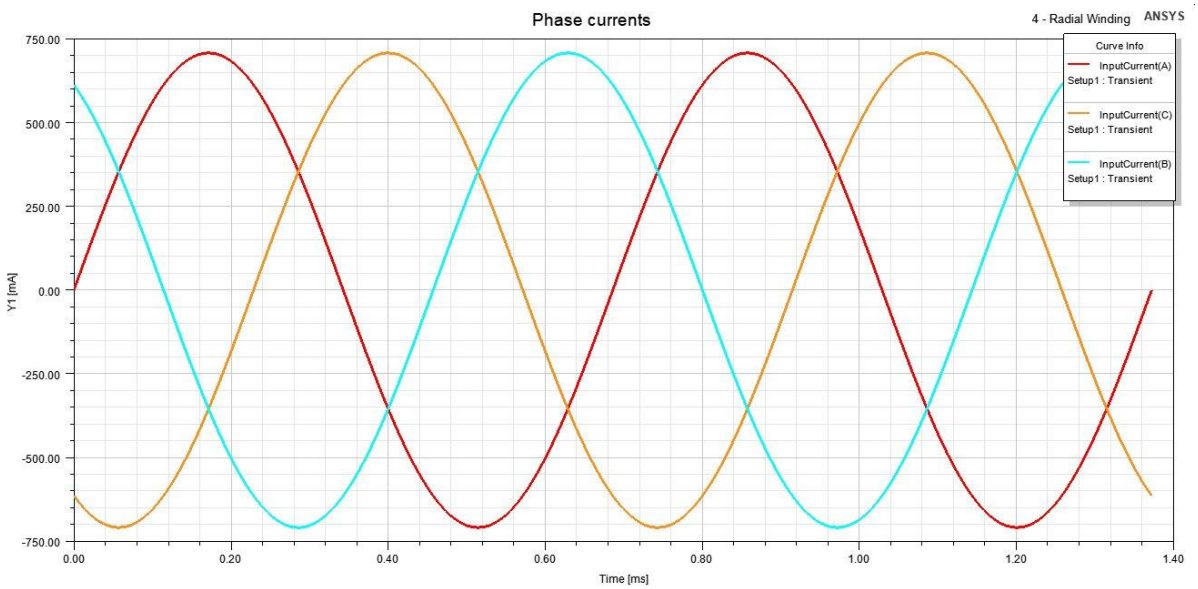

Figure 11. Input current waveforms of the motor.

The output torque is calculated as in Fig.12. There is no cogging torque in the motor since the motor is air-cored. Average torque value of 480 uN.m is achieved. The output torque is different than the calculated value. It may be because of the winding shape. In electrical loading calculation, there is no information about how the windings are positioned and what is the angle of the winding. These parameters closely affect the output torque. In radial-flux machines all windings are positioned without a skew. However, in wave windings created force vector is not in circumferential direction. The force vector should be multiplied with a cosine term in order to get the output torque value. So, torque calculation with electrical and magnetic loading may not be appropriate for axial-flux machines.

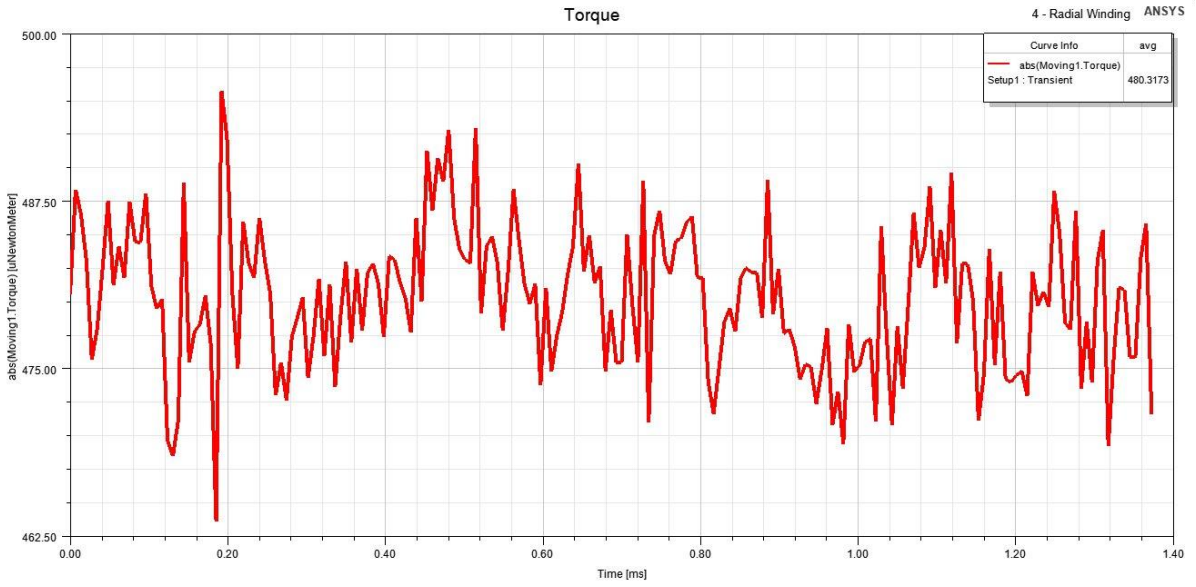

Figure 12. Created torque of the machine.

Copper loss of the machine is presented in Fig.13. The resistance of the path can be calculated from the loss value. It is found as 0.17 Ohm per phase. The average copper loss of the motor is found as 132 mW while the mechanical output power is

$$P_{mech} = T.\omega = 0{,}000480.1309 = 0.63\ W$$

Then, the efficiency of the motor as full-load can be calculated as

$$Efficiency_{full-load} = \frac{P_{mech}}{P_{mech} + P_{loss}} = 82.6\%$$

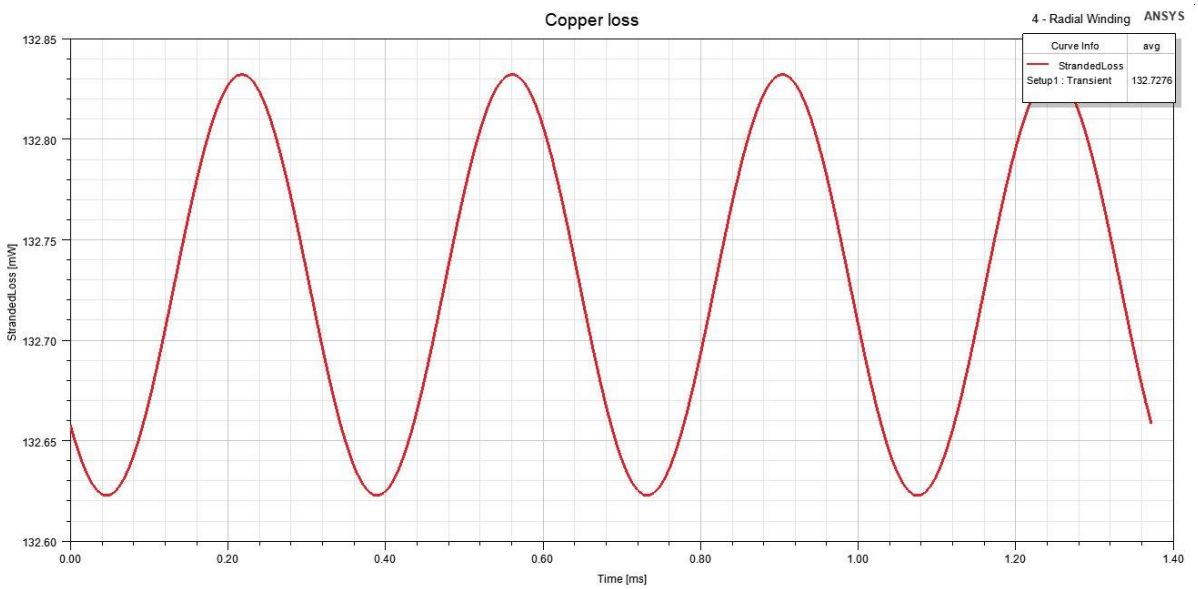

Figure 13. Copper loss of the windings.

Eddy loss of the motor is investigated since the speed of the motor is high. Eddy loss is found as in Fig.14. Since, I have used double rotor-single stator configuration, the eddy losses are negligibly small at uW range.

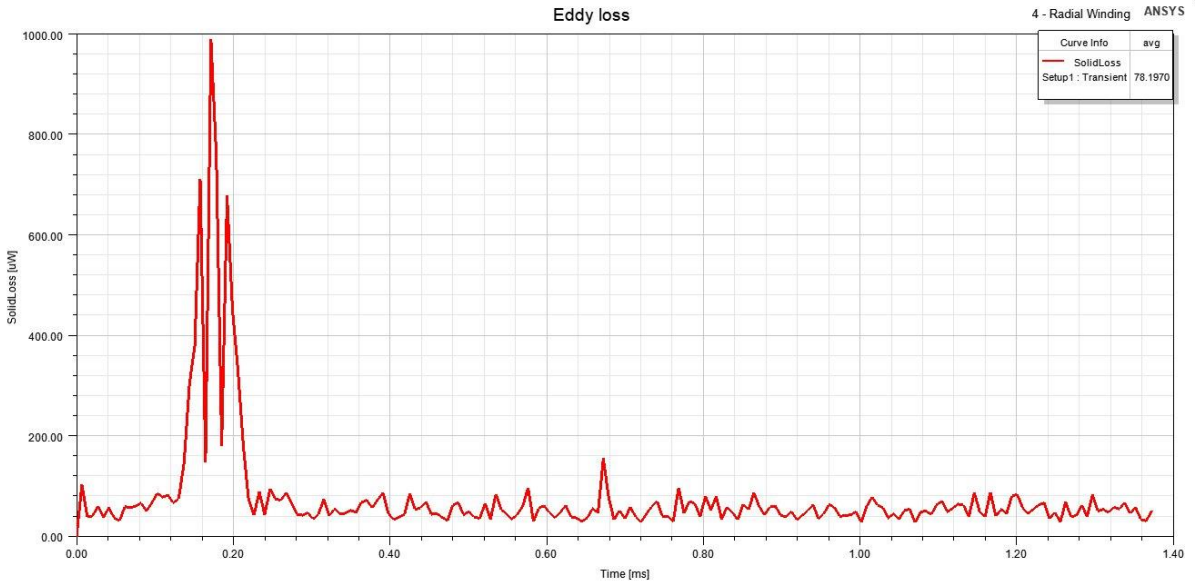

Figure 14. Eddy loss graph of the machine.

Direct axis and quadrature axis inductances of the machine is calculates using FEA. The results are presented in Fig.15. Since there no stator core, slot and teeth to create reluctance difference, direct and quadrature axis inductances are almost same.

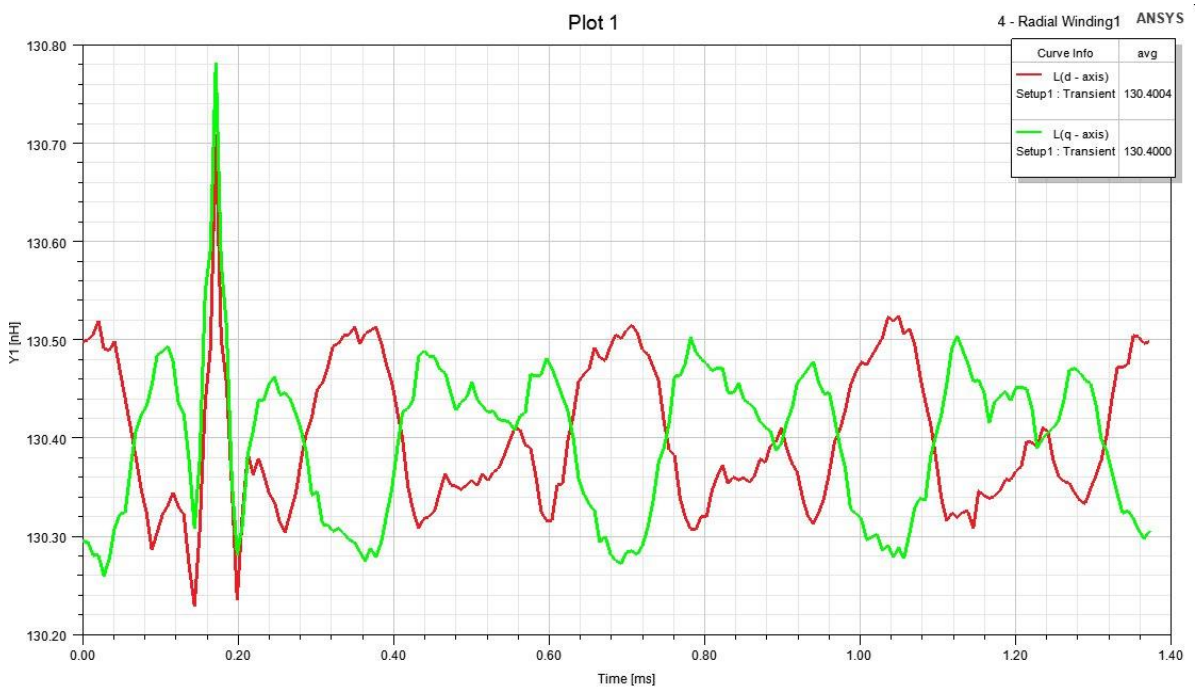

Figure 15. Direct and quadrature axis inductances of the machine.

4) Comparison & Discussion

In this project, I have designed an axial-flux permanent magnet synchronous machine with PCB winding. In order to find an application for the motor, I have investigated literature to find the spindle motor in [3]. This motor is a very small motor which is used in hard-disk drives. Axial-length of the motor should be small which makes axial-flux motor as a good alternative. Also, the outer diameter of the motor was 15.8 mm which makes the construction of these motor challenging. Using PCB winding in stator mitigates this problem. Axial-length of the constructed motor is 5 mm and aspect ratio 0.316. I have used steel back-cores with 0.6 mm thickness. The permanent magnets were N42 grade NdFeB magnets. Steel backplates weighs 1.54 gr. The magnets weigh 0.5 gr. If we neglect the weight of the PCB total weight of the motor becomes 2.04 gr. Torque density of the motor becomes

$$d_{torque} = \frac{T}{M} = \frac{0.000480}{0.00204} = 0.35\ N.m/kg$$

And the power density becomes

$$d_{power} = \frac{P_{mech}}{V_{motor}} = \frac{0.63}{0.000149} = 4221\ W/m^3$$

Output torque is very small and torque production is not the primary objective of spindle motors since they are expected to rotate in very high speed. So, high speed performance of the designed motor is investigated. The major problem in high speed -apart from mechanical problems- is that the eddy current losses. Since, the rotor is rotating in high speed, there will be eddy loss induced in the back plate of the single stator single rotor reference design. In order to eliminate these losses, I have used double rotor-single stator motor design. Thanks to that, there was no eddy losses in the rotor back plates.

Since, the motor is air-cored, there was no cogging torque. We can see this in direct and quadrature axis inductances. These inductances were almost the same. This proves that air-cored machines do not have reluctance torque.

If we compare the designed motor with the reference design, we can see that the main difference between two motors is the stator winding design. Rhomboidal winding was used in reference design. It resulted in back-emf constant of 0.107 mV/radsec with peak emf value of 0.2 V. I have used the unequal width radial winding topology in my motor. The main advantage of this configuration is that PCB surface area is better utilized. Thanks to radial winding, maximum torque that can be extracted from the motor is extracted. Also, unequal width winding ensures that the resistance of the path is minimal. We can see this result when we compare the reference design with the designed motor. The authors have ended up with 3 Ohm/m resistance in their design. I have found 1.06 Ohm/m resistance. Also, back-emf constant is found as 0.443 mV/radsec. So, we can say that unequal width radial winding is superior to its counterpart rhomboidal winding both in terms of induced voltage and resistance per phase. The THD levels of the induced voltage was not presented in the work. So, it is not possible to come to a certain conclusion from looking at the graph. But radial winding had 2.1% THD in induced phase voltage.

5) References

1. Z. Wen, B. Xiong, and G. Gu. Optimization design of low speed axial flux halbach permanent-magnet generator with pcb winding. In 2019 22nd International Conference on Electrical Machines and Systems (ICEMS), pages 1–4, 2019.

2. S. Moury and M. T. Iqbal. A permanent magnet generator with pcb stator for low speed marine current applications. In 2009 1st International Conference on the Developments in Renewable Energy Technology (ICDRET), pages 1–4, 2009.

3. M. . Tsai and L. . Hsu. Design of a miniature axial-flux spindle motor with rhomboidal pcb winding. IEEE Transactions on Magnetics, 42(10):3488–3490, 2006.

4. G. H. Jang and J. H. Chang. Development of an axial-gap spindle motor for computer hard disk drives using pcb winding and dual air gaps. IEEE Transactions on Magnetics, 38(5):3297–3299, 2002.

5. Ying-Chi Chuo, Chien-Chang Wang, Chien-Sheng Liu, Hsing-Cheng Yu, Yu-Hsiu Chang, and Ji-Bin Horng. Development of a miniature axial-field spindle motor. IEEE Transactions on Magnetics, 41(2):974–976, 2005.

6. G. H. Jang and J. H. Chang. Development of dual air gap printed coil bldc motor. IEEE Transactions on Magnetics, 35(3):1789–1792, 1999.

7. S. Paul, M. Farshadnia, A. Pouramin, J. Fletcher, and J. Chang. Comparative analysis of wave winding topologies and performance characteristics in ultra-thin printed circuit board axial-flux permanent magnet machine. IET Electric Power Applications, 13(5):694–701, 2019.

8. Parviainen, A. (2005). Design of axial-flux permanent-magnet low-speed machines and performance comparison between radial-flux and axial-flux machines.